Electronic Supplementary Material (ESI) for Physical Chemistry Chemical Physics.

Supplementary Materials for

Synergistic modulation of electrical and thermal transport toward promising n-type $MgOCuSbSe_2$ thermoelectric performance by MO-intercalated $CuSbSe_2$

Lingyun Ye[a], Liuming Wei[b, *], Yu Hao[b], Mengyan Ge[c], Xiaobo Shi[d], Hanxing Zhang[e, *]

[a]*Zhengzhou business University, Gongyi Henan 451200, China*

[b]*Department of Network Security, Henan Police College, Zhengzhou 450046, China*

[c]*Department of Physics, College of Sciences, Nanjing Agricultural University, Nanjing 210095, China*

[d]*Henan Finance University, Zhengzhou 450046, China*

[e]*Department of Electronics and Information Technology, Anhui University of Finance and Economics, Bengbu 233030, China*

**Corresponding authors*

Emails: lmwei@theory.issp.ac.cn and hxzhang@theory.issp.ac.cn

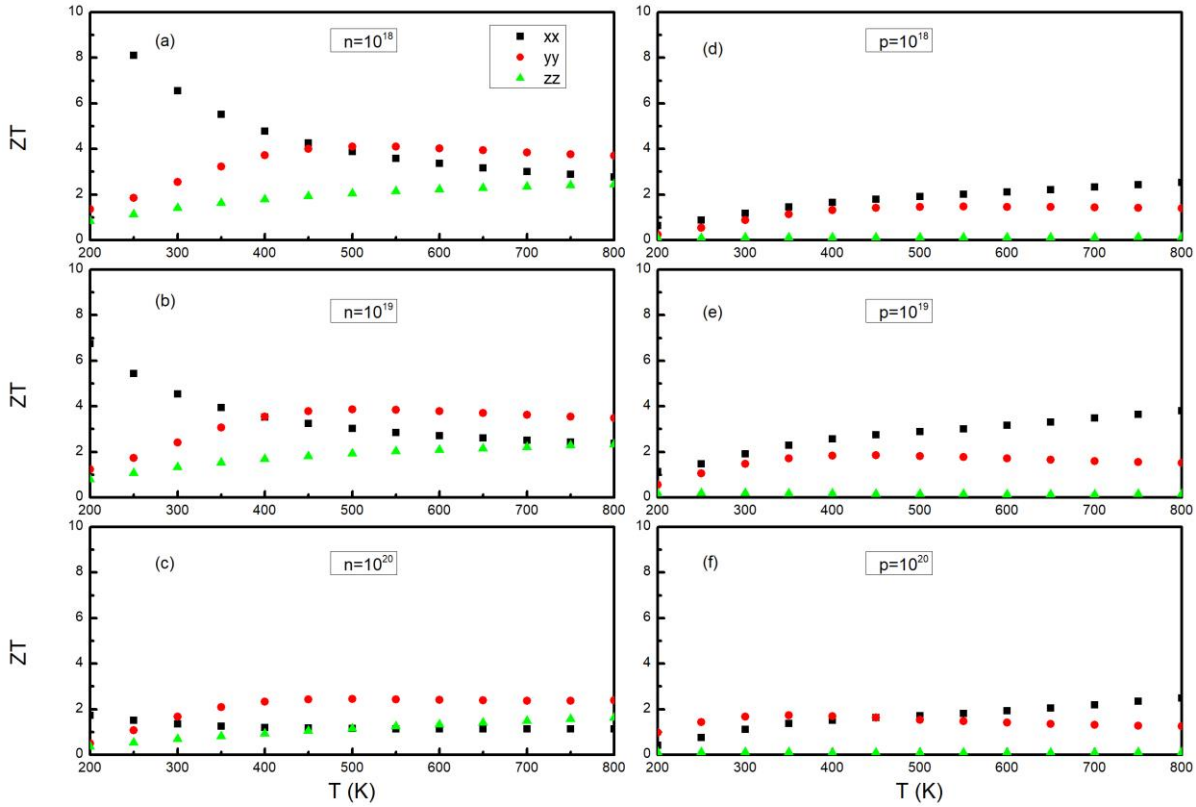

Fig. S1. Calculated temperature dependence of the anisotropic figure of merit ZT of $MgOCuSbSe_2$ as functions of carrier concentration at 10^{18}, 10^{19}, and 10^{20} cm^{-3} for n-type doping (left panels) or p-type doping (right panels).

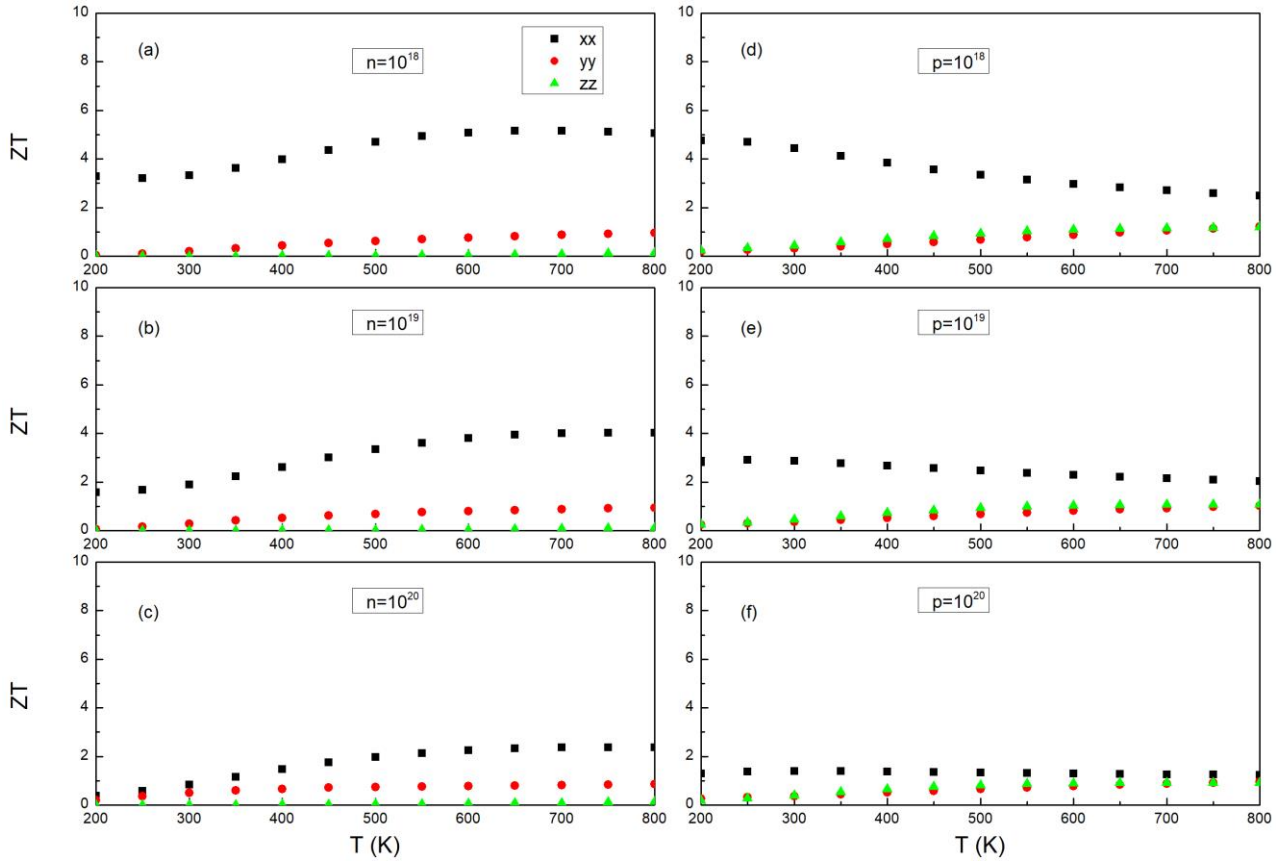

Fig. S2. Calculated temperature dependence of the anisotropic figure of merit ZT of $CaOCuSbSe_2$ as functions of carrier concentration at 10^{18}, 10^{19}, and 10^{20} cm-3 for n-type doping (left panels) or p-type doping (right panels).

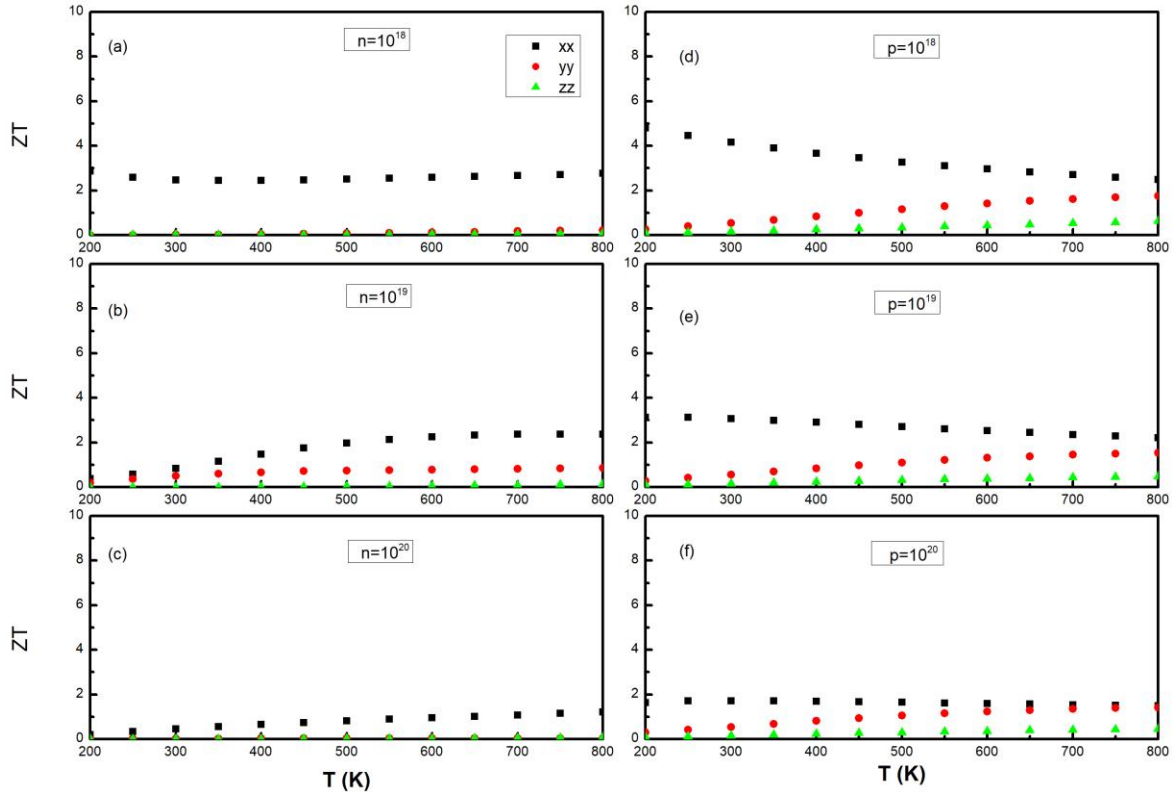

Fig. S3. Calculated temperature dependence of the anisotropic figure of merit ZT of $SrOCuSbSe_2$ as functions of carrier concentration at 10^{18}, 10^{19}, and 10^{20} cm-3 for n-type doping (left panels) or p-type doping (right panels).

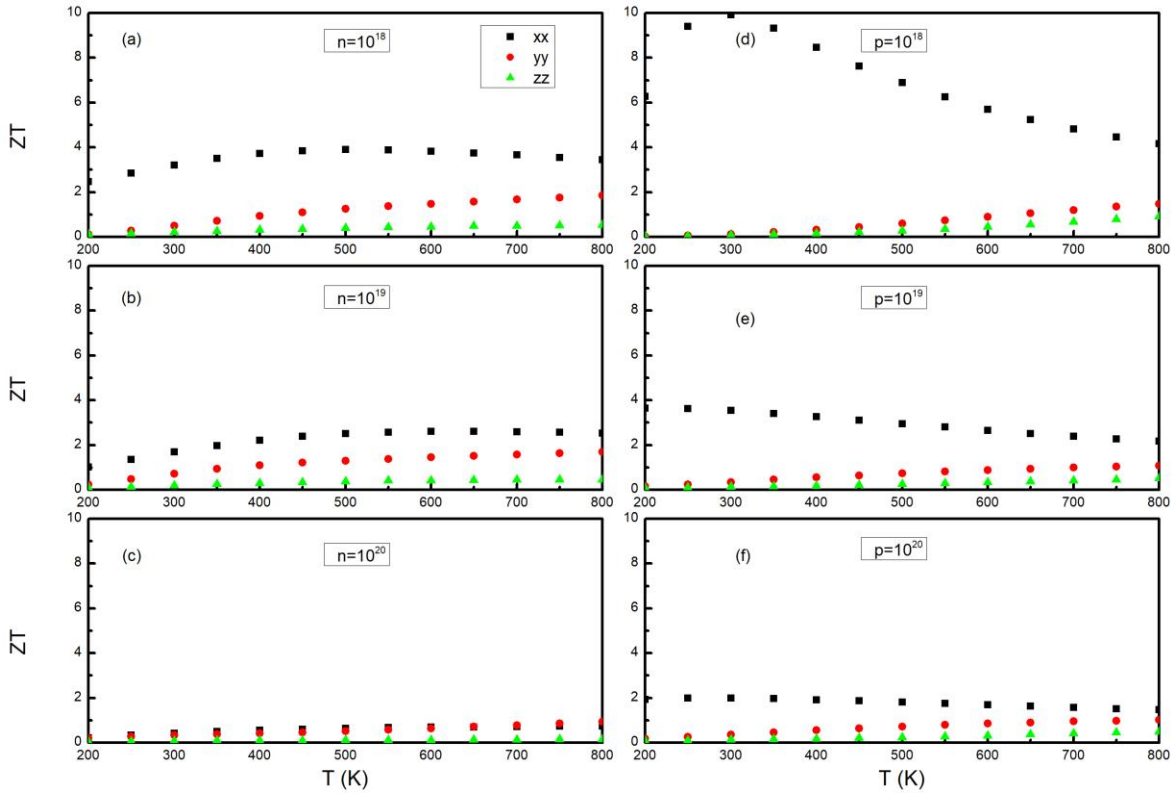

Fig. S4. Calculated temperature dependence of the anisotropic figure of merit ZT of $BaOCuSbSe_2$ as functions of carrier concentration at 10^{18}, 10^{19}, and 10^{20} cm^{-3} for n-type doping (left panels) or p-type doping (right panels).

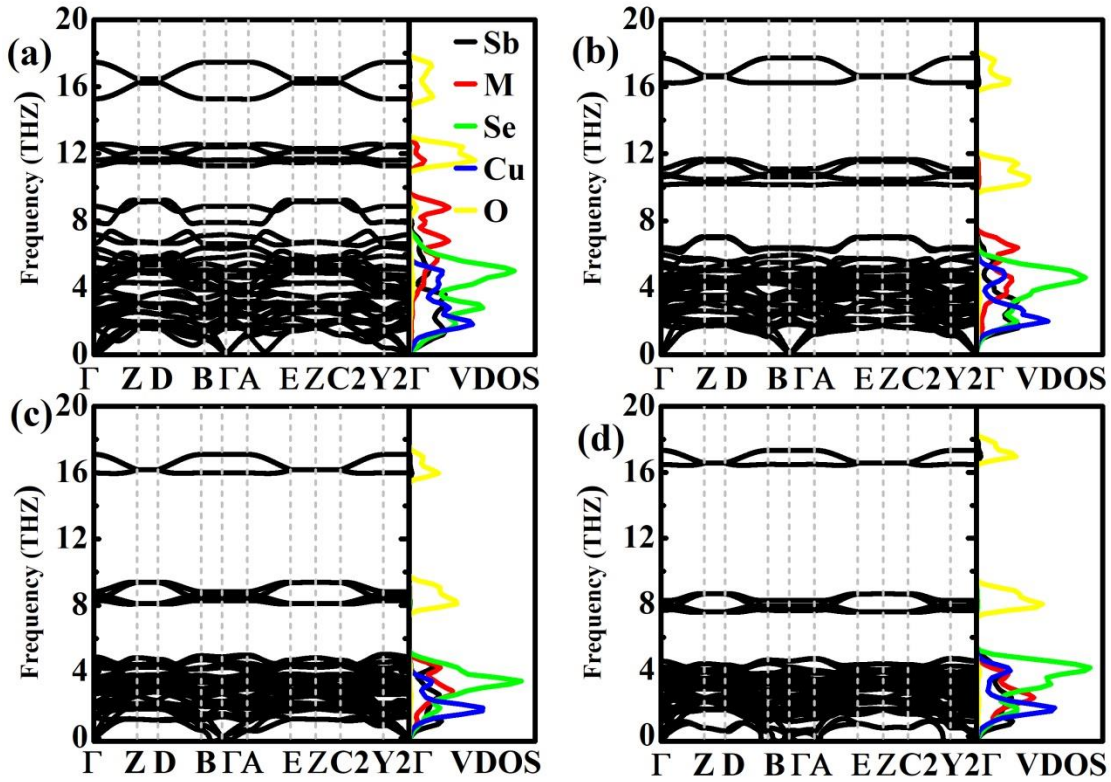

Fig. S5 The full spectra phonon band structures and vibrational density of states for (a) $MgOCuSbSe_2$, (b) $CaOCuSbSe_2$, (c) $SrOCuSbSe_2$, and (d) $BaOCuSbSe_2$.

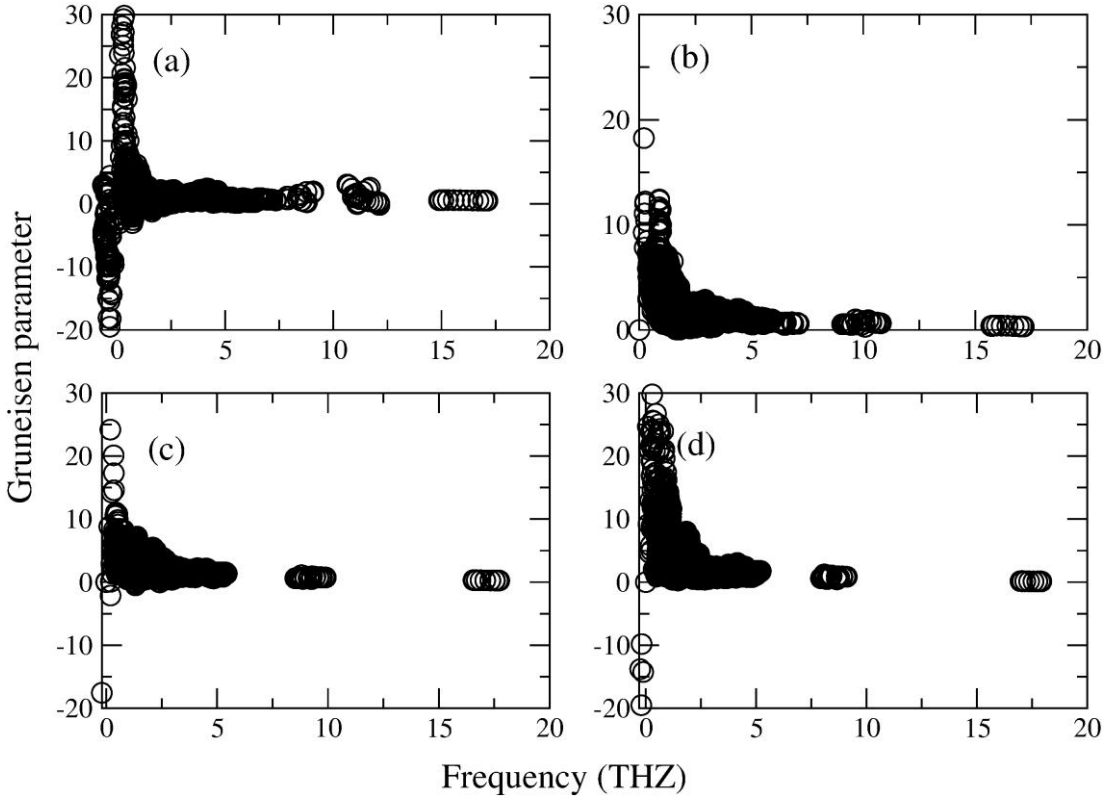

Fig. S6. Calculated frequency-dependent Grüneisen parameters of for (a) $MgOCuSbSe_2$, (b) $CaOCuSbSe_2$, (c) $SrOCuSbSe_2$, and (d) $BaOCuSbSe_2$.

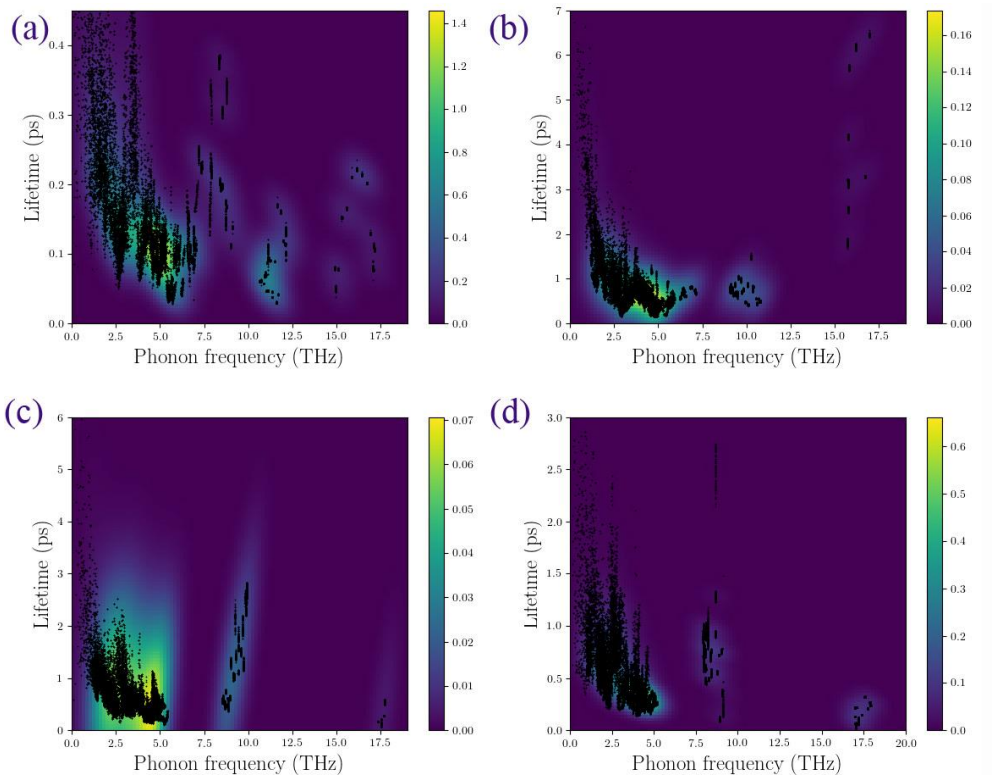

Fig. S7. Calculated phonon relaxation time for (a) $MgOCuSbSe_2$, (b) $CaOCuSbSe_2$, (c) $SrOCuSbSe_2$, and (d) $BaOCuSbSe_2$.

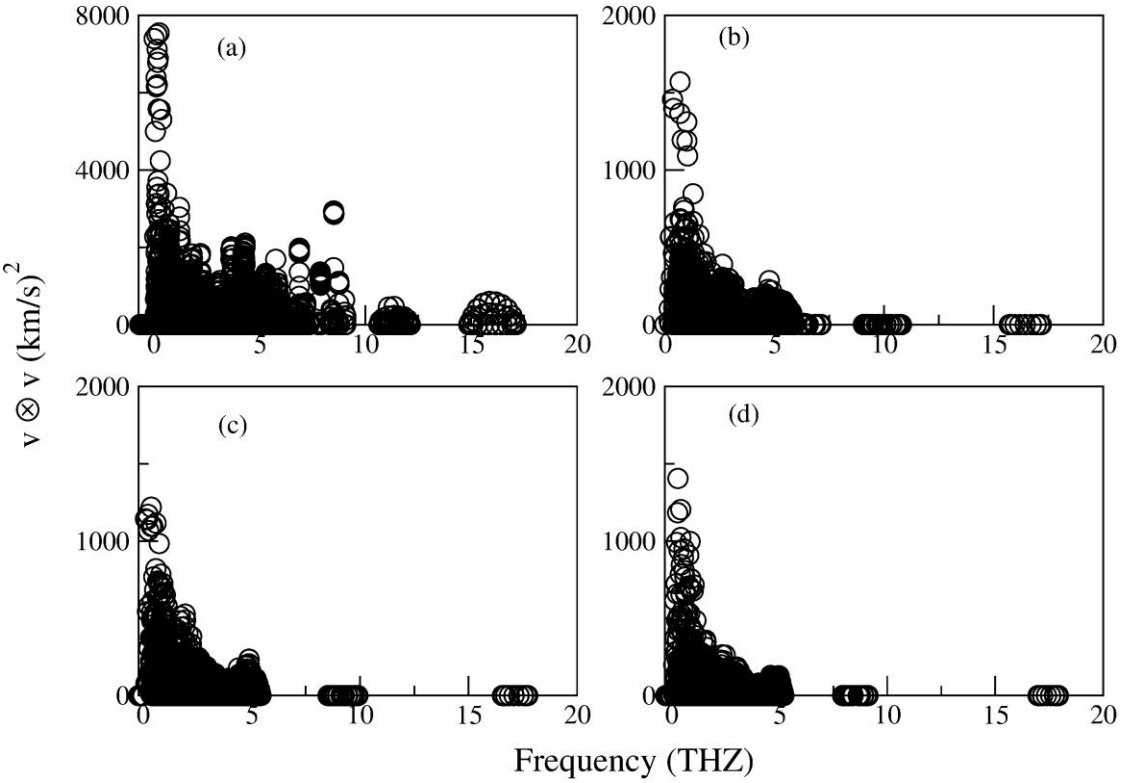

Fig. S8. Calculated square group velocity as a function of frequency for (a) $MgOCuSbSe_2$, (b) $CaOCuSbSe_2$, (c) $SrOCuSbSe_2$, and (d) $BaOCuSbSe_2$.